OMAE2004-51153

BEARING BEHAVIOUR OF SPUDCAN FOUNDATION ON UNIFORM CLAY DURING DEEP PENETRATION

M.S. Hossain
Department of Civil Engineering
Curtin University of Technology
Western Australia 6845, Australia
Email: hossainm@vesta.curtin.edu.au

Y. Hu
Department of Civil Engineering
Curtin University of Technology
Western Australia 6845, Australia
Email: yuxia@vesta.curtin.edu.au

M.F. Randolph
Centre for Offshore Foundation Systems
The University of Western Australia
Western Australia 6009, Australia
Email: randolph@civil.uwa.edu.au

ABSTRACT

In order to design a safe spudcan foundation, it is important to predict its bearing behaviour accurately based on the corresponding soil failure mechanisms. Thus, the performance of spudcan foundation, during deep penetration into uniform soil, is investigated physically and numerically. In physical testing, a series of centrifuge tests are carried out in a drum centrifuge. The half-spudcan model tests with subsequent Particle Image Velocimetry (PIV) analysis are conducted to reveal soil failure mechanisms during spudcan penetration. And the full spudcan model tests are conducted to investigate the bearing capacity of spudcan. In numerical simulation, FE analyses are performed considering smooth and rough soil-spudcan interface. From the physical tests and numerical analyses, it is observed that the cavity is formed above the spudcan as it is penetrating into uniform clay. At certain penetration depths, the soil underneath the spudcan starts to flow back on top of the spudcan, which leads the spudcan to be embedded with further penetration. Soil flow mechanisms, at various penetration depths, play a key role in footing bearing response. And the ultimate undrained bearing capacity factor of $N_c = 10.5$ (smooth) and 12 (rough) are obtained at deep penetration.

Keywords: Spudcan, Deep Penetration, PIV analysis, Failure Mechanisms, Bearing Capacity Factor, Uniform Clay.

INTRODUCTION

Jack-up rigs are widely used in offshore oil and gas exploration and increasingly in temporary production and maintenance work. Whilst originally designed for use in relatively shallow water depths, due to their economic importance within the offshore industry, there has been a steady increase in demand for their use in deeper water, up to 120 m, and harsher environment [1]. Most jack-up units currently use circular conical footings known as spudcans (Fig. 1) as their foundations.
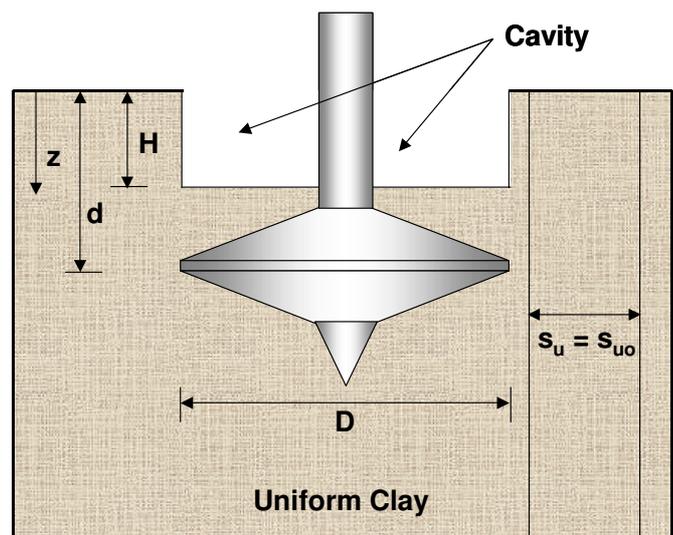
Figure 1 - Spudcan foundation in uniform clay

Before the commencement of the jack-up operation, the spudcans are preloaded by pumping seawater into the hull. The

1   Copyright © 2004 by ASME

preload causes the spudcans to penetrate into the seabed until the load on the spudcan is equilibrated by the resistance of the underlying soil. In soft soil, spudcan could penetrate up to 2-3 diameters to be equilibrated. The purpose of preloading is to prestress the foundation so that it's resulting bearing capacity exceeds the anticipated extreme storm loading by an acceptable margin of safety. For a 50-year design storm, a common practice is to preload the foundation to twice the working vertical load. The ballast is then discharged and the hull is raised further to provide adequate air-gap between the hull and the water surface for subsequent operation. During initial preloading, and in calm weather, the footings of a jack-up are essentially subjected to purely vertical loading. To date, the major causes of jack-up failure are soil related [2,3] which usually occurs during installation. Although 'punch-through' failure, in which a foundation can penetrate into soil a great distance in a short time, usually occurs in layered soil deposits, failures on homogeneous clay are also quite often [4]. It should be noted that jack-up rig failure caused loss not only of economy of about US$90 million but also of lives.

Bearing behaviour of spudcan foundation subjected to vertical loading on uniform clay is continually being assessed from centrifuge testing. Soil flow mechanisms were depicted by some investigators. For instance Craig and Chua [5,6] endeavoured to visualise soil failure mechanisms by inserting dry spaghetti markers vertically in the soil across the centerline of the foundation position. However, these illustrations display only the ultimate soil failure mechanisms. Hossain et al. [7] depicted clearly the varying soil failure mechanisms up to deep penetration from centrifuge model tests, but the image quality was low as they were captured by a low resolution video camera upon the grid drawn on soils. 'Line jitter' and the transmission of the analogue video signal through centrifuge sliprings further reduced image quality.

The literature dealing with bearing response of spudcan footing is quite extensive. Dean et al. [8] performed model tests with three-leg jack-up. Craig and Chua [5,6] and Hossain et al. [7] presented the bearing capacity of a single spudcan in clay of different strength. However, most of the experiments were limited either to shallow depth assuming that the displacement of the spudcan prior to attaining the ultimate load is very small or the effect of soil flow mechanisms on the bearing response has not been fully explored.

The spudcan bearing behaviour has also been extensively investigated from upper bound, lower bound and FE analysis. Some research on circular flat-plate could tacitly be considered as a simplified spudcan foundation. Martin and Randolph [9] reported upper and lower bound analyses for surface and buried flat plate circular foundation, showing the predicted soil collapse mechanisms and corresponding bearing capacity factors (N_c). This study did not intend to extend to continuous penetration.

Hossain et al. [7] have discussed soil flow mechanisms and bearing capacity factor considering footing roughness. However, in the analysis, cavity above the footing top was modelled as fully open and fully embedded and thus the effect of soil back flow has been neglected.

More recently Houlsby and Martin [10] have presented the bearing capacity factors of foundation from lower bound analysis. The footing was modelled as a cone and the corresponding values of the dimensionless bearing capacity factor N_c were presented in a tabulated form as a function of the cone angle, cone roughness, depth of embedment and the rate of increase of strength with depth of the clay. However, in all analyses the soil was assumed to be weightless. Furthermore, it was assumed that the space above the footing was occupied by a rigid, smooth-sided shaft. Therefore, the results would not be applicable to the case of spudcan foundation penetration where soil will flow back on top of the footing.

At typical offshore soft clay sites, deep spudcan installation is usually associated with a substantial amount of back flow [11,12]. Soil back flow might be occurred due to (i) plastic flow around the spudcan edge, or (ii) collapse of upstanding soil on the cavity wall into the hole, or (iii) both. Since the back flow occurs at a certain depth, a cavity can be formed, especially in an overconsolidated soil site. The bearing capacity estimation can be affected by the cavity formation. Thus in this paper, the cavity formation mechanism, cavity depth and bearing capacity are studied together to provide further understanding on the bearing behaviour of spudcan foundation during its deep penetration.

CENTRIFUGE TESTING

The experimental investigation was conducted in the drum centrifuge located at the University of Western Australia (UWA), which has a diameter of 1.2 m and maximum acceleration level of 485 g. Technical details of the drum centrifuge can be found in Stewart et al. [13]. A special strong box (258 × 80 × 160 mm) with a plexiglass window was built to allow visualisation of soil flow mechanisms through the window. Soil flow images were captured by a high resolution (2270 × 1704 pixels) digital still camera. All experimental set-ups are shown in Fig. 2.

Figure 2 - View of drum channel set-up

In order to obtain data close to the offshore field situation, water was sprinkled over the soil specimen through a nylon

2   Copyright © 2004 by ASME

hosepipe at a lower acceleration level (15 g) to avoid injection induced distortion. A free water depth of about 30 mm was maintained above soil surface during testing.

In this study, a half-spudcan of 60 mm dia and a full-spudcan of 30 mm dia model, made from dural, were used with a 13° shallow conical underside profile and a 76° protruding spigot (Fig. 3). The self-weight of the full-spudcan model is about 0.04 kg.
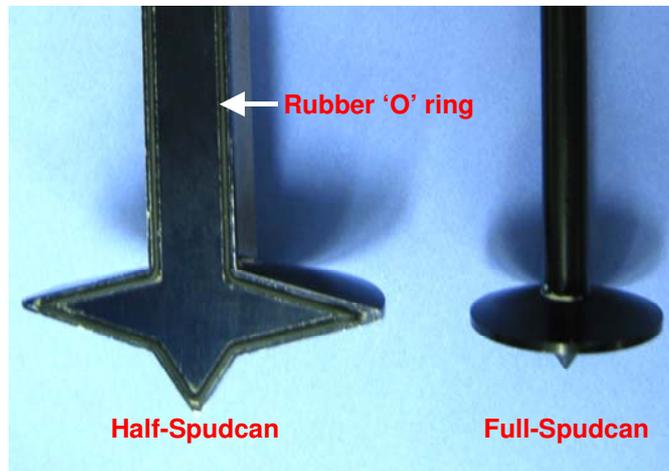
Figure 3 - Spudcan models

In offshore fields, jack-up preloading on soft clays frequently leads to spudcan penetrations up to 2-3 diameters [11], thus the experimental work here covered a similar range of penetration. All experimental investigations discussed in this article were carried out at 100 g. The relevant scaling relationships for modelling at elevated accelerations are shown in Table 1. All results in this paper are presented in terms of prototype units.

Table 1 - Scaling relationship used during centrifuge modelling

Parameter	Scaling Relationship (model / prototype)
Gravity	N
Stress	1
Strain	1
Length	1/N
Force	$1/N^2$
Density	1
Mass	$1/N^3$
Velocity	N
Time (consolidation)	$1/N^2$

NUMERICAL MODELLING

Numerical analyses were conducted using the AFENA finite element package developed by Carter & Balaam [14]. *H*-adaptive mesh generation [15] has ensured that an optimal mesh was generated. Spudcans of diameter 6 m and 12 m with smooth and rough soil-spudcan interfaces were considered. These were to assess the effect of footing size and roughness on its bearing response. Figure 4 shows the geometry and

dimensions of spudcan with 6 m in diameter. All the dimensions were doubled for spudcan with 12 m in diameter. The soil domain was 12 D in width and 20 D in depth where half space was analysed due to axisymmetry.
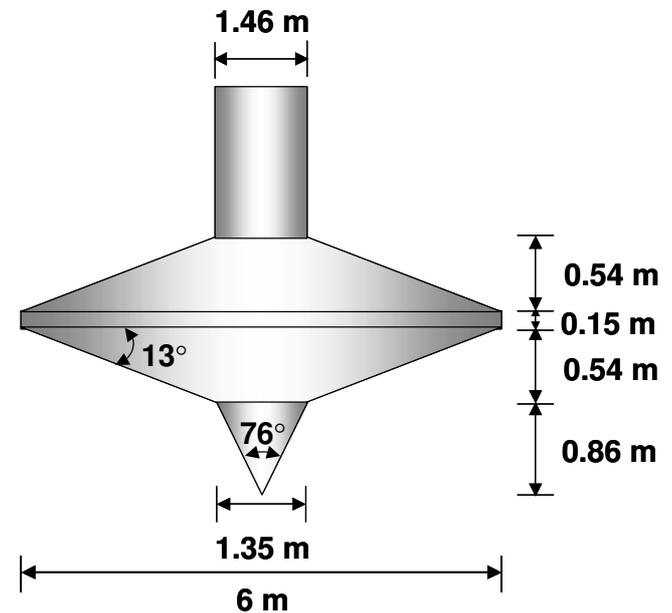
Figure 4 - Geometry of spudcan

The soil was modelled as elasto-plastic material with Tresca yield criterion. All the analyses simulated undrained conditions and hence Poison's ratio $\nu = 0.49$, the friction and dilation angles $\phi = \psi = 0$, and the uniform stiffness ratio $E/s_u = 500$ (where E is Young's modulus and s_u is the undrained shear strength) were considered. In small-strain bearing capacity analyses, pre-embedment ratios (d/D in Fig. 1) were varied from 0.025 to 2.76. To simulate the saturated deposit submerged under water, soil unit weight of $\gamma = 7$ kN/m³ was considered in total stress analysis. The uniform undrained shear strength of $s_u = 12$ kPa and 18 kPa were chosen. To ensure the accuracy of the FE analyses, the minimum element size (h_{min}) and displacement increment (δ) were selected using following criteria [15]:

$$h_{min} = 0.005D \quad (1)$$

$$\left(\frac{\delta}{D}\frac{E}{s_u}\right) * \left(\frac{kD}{s_{u0}}\right)^{0.8} = 0.03 \quad (2)$$

where *k* is the gradient of s_u with depth. Although $k = 0$ for uniform soil, kD/s_{u0} was taken as one for uniform soil. And undrained shear strength at soil surface $s_u = s_{u0}$.

3   Copyright © 2004 by ASME

RESULTS AND ANALYSIS

Soil Strength Profile

Kaolin clay was used in the centrifuge modelling, with the key properties shown in Table 2. This clay has been used in many laboratory investigations at UWA and so has been well studied.

Table 2 - Kaolin clay properties (after Stewart [16])

Property	Value
Liquid Limit, LL	61 %
Plastic Limit, PL	27 %
Plasticity Index, I_p	34 %
Specific Gravity, G_s	2.6
Consolidation Coefficient, c_v	2 m^2/year

Soil was consolidated into a conventional consolidation tank in standard manner under a maximum pressure of 150 kPa. After full consolidation, the soil sample was removed from the tank and trimmed into test specimens with equal size of the strong box with $258 \times 80 \times 120$ mm dimensions. The details of sample preparation can be found in Hossain et al. [7].

Soil characterisation tests were performed using a T-bar penetrometer [17]. These tests were performed at a rate of 1 mm/s so that undrained behaviour was obtained [18]. A typical undrained shear strength profile is illustrated in Fig. 5. The vertical axis z represents the soil depth in prototype. It can be seen that the soil strength is fairly uniform for z > 4 m. The softer soil at z < 4 m is due to the presence of water layer on top of the soil, which caused the softening effect.
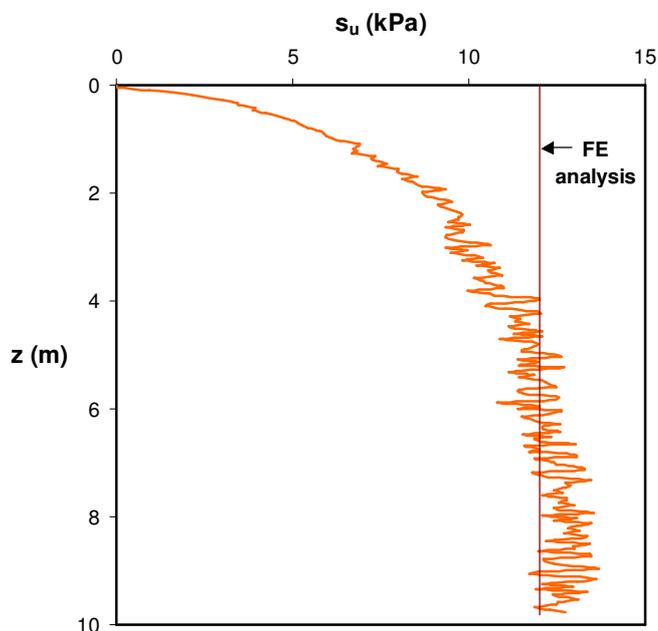
Figure 5 - Undrained shear strength profile of submerged OC clay

Soil Flow

The half-spudcan was penetrated into the soil (of strength as shown in Fig. 5) with the central flat side placed tightly against the window to prevent soil particles ingress between the window and the spudcan model. Tests were run at a comparatively lower penetration rate of 0.05 mm/sec to track the soil deformation more precisely. Nonetheless, an undrained behaviour was maintained [18]. The black 'flock' modelling material was sprinkled on the soil specimen side facing the window so that the images captured by the digital camera could be used for subsequent Particle Image Velocimetry (PIV) analysis [19]. Soil flow images were captured continuously by a digital camera facing at right angles towards the midheight of the window. PIV operates by tracking the texture (i.e. the spatial variation of brightness) within an image of soil through a series of images. The initial image is divided up into a mesh of PIV test patches. The displaced location of each patch in a subsequent image is obtained by determining the location of highest correlation between each patch and a large search region from a following image. Although the correlation plane is evaluated at single pixel intervals, by fitting a bicubic interpolation to the region close to the integer peak, the displacement vector is established to sub-pixel resolution. Eventually, photogrammetry was applied to convert the displacement vectors measured by PIV from image-space (pixels) into object-space (mm) instead of a single scaling factor.

Figure 6 illustrates the digital images at various penetration depths. As spudcan penetrated into uniform clay, soil heaved up towards the surface, thus a cavity was formed. (Fig. 6(a)). With further penetration, soil started to flow back on the exposed top of the spudcan (Fig. 6(b)). At deep penetration, the spudcan became fully embedded, while the cavity formed during initial penetration was kept open (Fig. 6(c)). This indicates that the soil flow has become localised without the effect to the soil surface profile. Therefore, the cavity depth (H) can be measured.

(a) soil heave
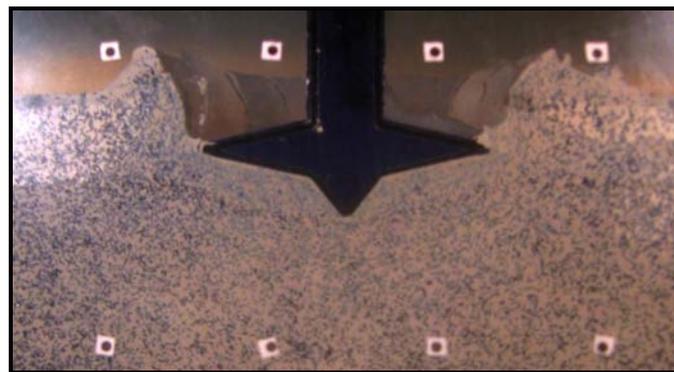
4   Copyright © 2004 by ASME
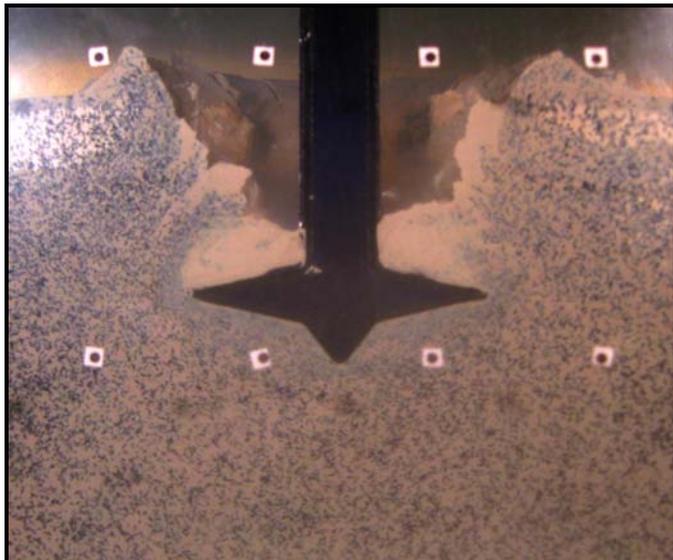
(b) soil back flow
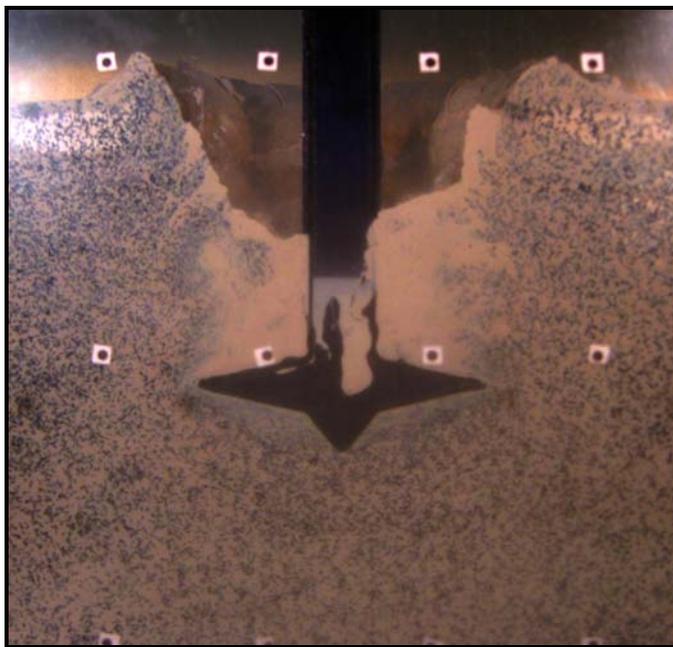
(c) deep foundation
Figure 6 – Digital images during half-spudcan penetration in centrifuge test

Figure 7 shows the corresponding soil displacement vectors from the results of PIV analysis. Figure 7(a) displays the classical feature of a general bearing capacity failure. It can be seen that a significant amount of soil underneath the spigot (0.8 D) moves downward with the spudcan and the soil around spudcan edge shows a transitional movement from laterally to vertically upward. At deep penetration (Figs. 7(b) and 7(c)) with spudcan fully embedded in soil, however, the region of soil moving downwards decreases to 0.5 D, thus more soil shows a transitional movement around the spudcan edges. The lateral deformation zone has a region of 1.5~1.6 D for surface footing and of 1.3~1.4 D for deeply penetrated footing. It should be noted that the empty parts above the spudcan in Figs.

7(b) and 7(c) are not cavities. The lack of vectors is due to the lack of "flock" in the back-flow soils.
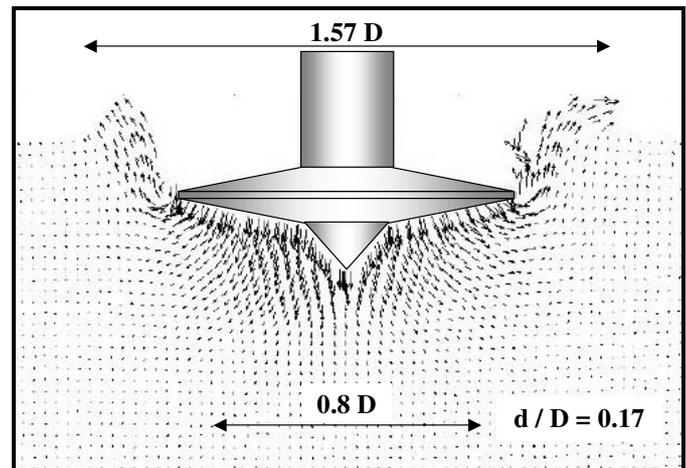
(a) surface flow
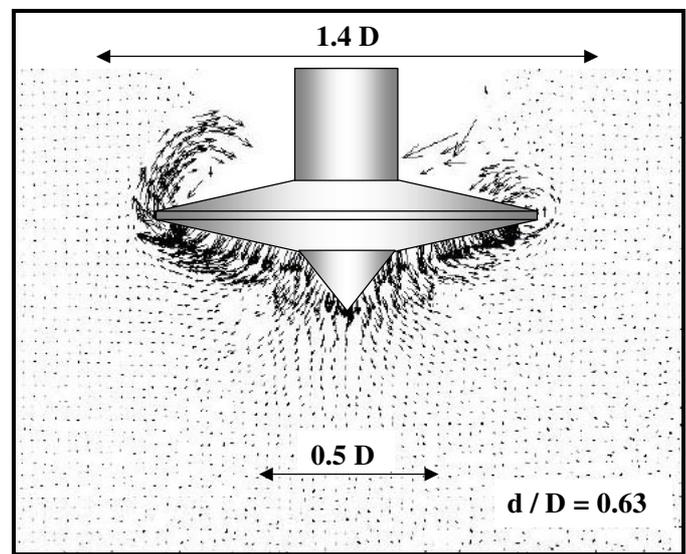
(b) back flow
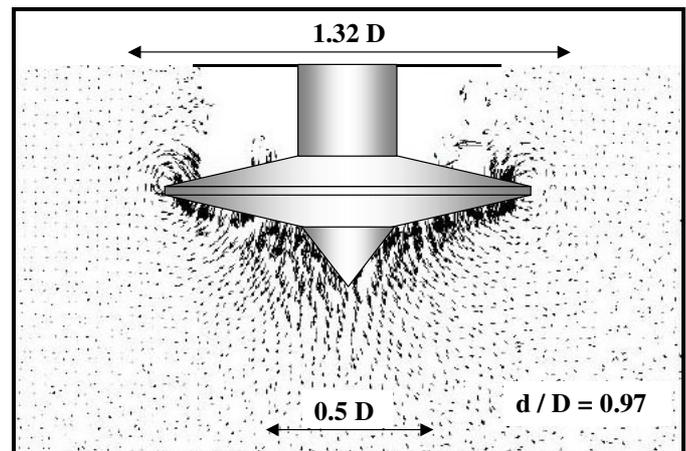
(c) local flow
Figure 7 – Soil flow mechanisms in centrifuge test from PIV analysis

5   Copyright © 2004 by ASME

Figure 8 depicts soil flow mechanisms from FE analyses, with a smooth spudcan of 6 m diameter. It can be seen that the soil failure mechanisms are entirely similar to the ones from centrifuge test results (Fig. 7). The cavity formed above the spudcan remains open up to a depth (H) till soil starts to flow back on top of the spudcan. In addition, the lateral distortion zone of soil extends well up to about 1.7 D for surface footing and about 1.6 D for deeply embedded footing, which agrees very well with the centrifuge observation (Fig. 7).
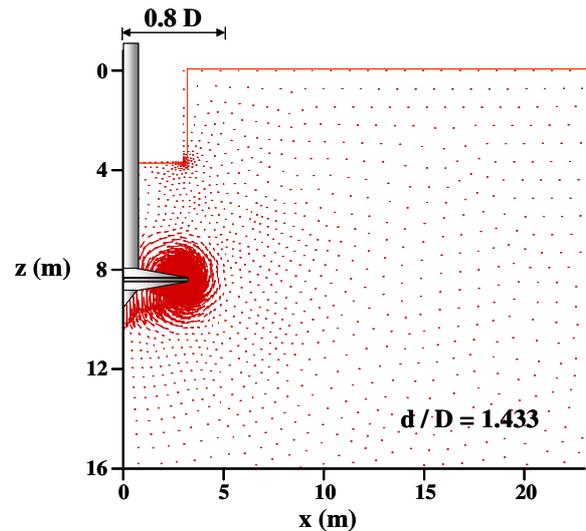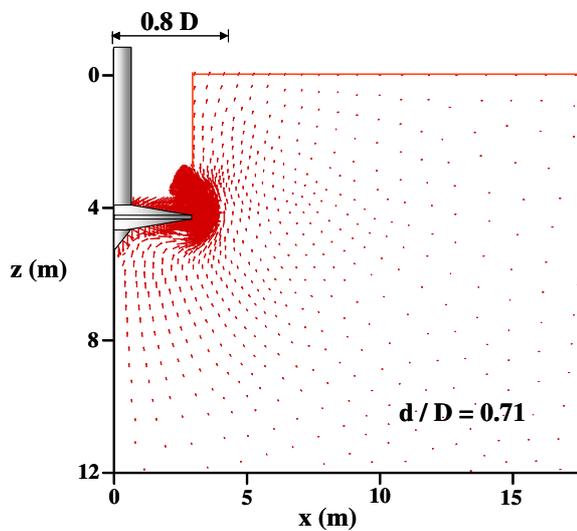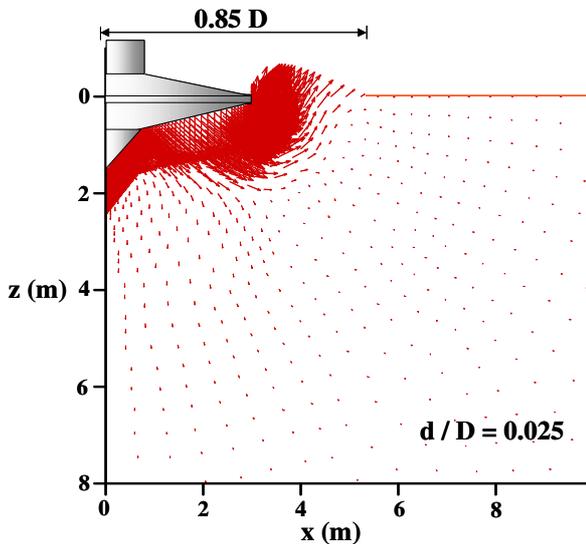
Figure 8 - Soil failure mechanisms from FE analysis

However, the open cavity depth H is obtained as 3.6 m in FE analysis and 2.8 m in centrifuge test. This can be due to the lower strength with softer surface soil in centrifuge test (Fig. 5). This clearly demonstrates that the depth of stable cavity above the spudcan depends significantly on soil strength. Table 3 shows all the measured values of cavity depth study with a non-dimensional factor – stability number $\gamma D/s_u$. In all cases the soil unit weight $\gamma = 7$ kN/m^3 was used in $\gamma D/s_u$ calculation. From Table 3, it can clearly be seen that with all different cavity depths and spudcan diameters, the cavity depth ratio (H/D) is decreasing with increasing the stability number.

Table 3 - Cavity depth in centrifuge tests and FE analyses

D (m)	s_u (kPa)	$\gamma D/s_u$	H/D
3	12	1.75	0.73
6	18	2.33	0.60
6	12	3.50	0.48
12	18	4.67	0.43

Bearing Capacity

Bearing capacity of spudcan foundation, during deep penetration, has been extensively assessed from centrifuge tests and FE analyses. In centrifuge tests, the full-spudcan penetration tests were carried out (at 100 g) to measure load-penetration response. Tests were performed along the centre of the soil specimen to avoid the boundary effect from the strongbox. A constant penetration rate was 0.2 mm/sec, thus undrained condition was maintained [18].

In this study, the bearing capacity results from centrifuge test and FE analyses are presented as the dimensionless bearing capacity factor, N_c, which is calculated under undrained penetration as

$$N_c = \frac{q_u}{s_u} \tag{3}$$

6   Copyright © 2004 by ASME

where q_u is the net ultimate bearing pressure on spudcan foundation.

Figure 9 summarises all the N_c values from centrifuge test and FE analyses. The centrifuge result is for spudcan of diameter 3 m and soil strength as shown in Fig. 5. And FE results are for spudcan of diameter 6 m and 12 m with both smooth and rough interface. Basically, which were to compare soil flow mechanisms with half-spudcan centrifuge tests. This Figure presents the effects on the spudcan bearing response from soil flow mechanism, cavity depth, footing size and footing roughness.
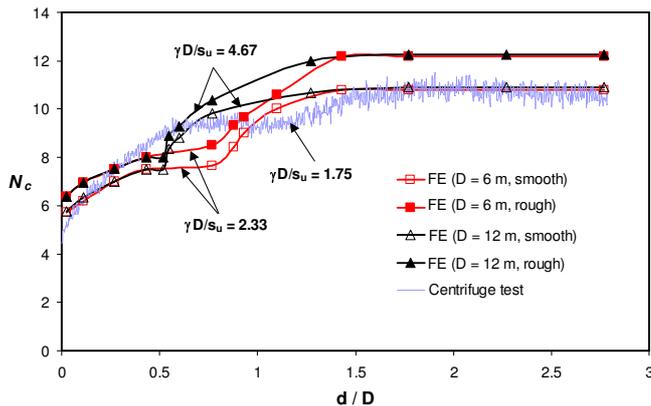
Figure 9 - Bearing capacity factor, N_c of spudcan on uniform clay

It can be seen that N_c values increase initially due to the cavity formation, which adds surcharge on the surface foundation (Figs. 6(a), 7(a) and 8(a)). This increase slows down and reaches the first plateau. This indicates the soil back flow, which reduces the increasing surcharge effect due to open cavity (Figs. 6(b), 7(b) and 8(b)). After this plateau, the N_c values increase sharply again until they reach the final stable values. This can be explained as the bearing capacity of spudcan increases while the soil flow changes from shallow mechanism to deep mechanism. When the final stable N_c number is achieved, the soil flow is stabilised at deep embedment mechanism (Figs. 7 (c) and 8(c)), where the flow mechanism around spudcan has no effect on the soil surface profile. From the curves in Fig. 9, all show the characteristics of first plateau and final stable values of N_c number. However, they reach the same stages at different penetration d/D ratios. This coincides with the cavity depth ratio H/D with different $\gamma D/s_u$ situations in Table 3.

Despite the different ways of reaching the final stable N_c numbers, they all converge to a same value for the smooth and rough interface respectively. The centrifuge test result agrees well with the FE results of smooth interface with an identical limit number of $N_c = 10.5$ reached. This is due to the sufficiently polished spudcan was used in centrifuge testing. In FE analysis, the rough soil-spudcan interface shows about 14% higher result than the one for the smooth interface.

CONCLUSIONS

This paper describes the results of drum centrifuge testing and FE analyses aiming to assess the performance of spudcan foundation on uniform clay during deep penetration. Bearing capacity based on revealed soil failure mechanisms has been discussed. The actual undrained bearing behaviour of spudcan foundation subjected to the vertical monotonic loading is related to the preloading of jack-up during installation. Several concluding comments are summarized below.

As spudcan penetrated into uniform clay, a stable cavity was formed and soil flowed plastically from spudcan base to the soil surface. Thus, soil heave was formed close to the footing edges. With further penetration, soil started to flow back on the exposed top of the spudcan. The stable open cavity depth ratio (H/D) is decreasing with increasing the stability number $\gamma D/s_u$. A full relationship between the stability number and the stable cavity depth is being studied and will be published in a subsequent paper. The cavity depth from FE analysis is greater than the one in centrifuge observation. This is because that the uniform strength profile in FE analysis provides a stronger top soil layer than the one measured in centrifuge. At deep penetration, when the spudcan is fully embedded, the flow mechanism is localised around the spudcan.

From PIV analysis of the centrifuge images and FE results, it can be observed that there are three stages during deep penetration of spudcan foundation into uniform soil: (1) at shallow penetration, soil heave and cavity are formed. The lateral distortion of soil field is in the region of 1.5 ~ 1.6 D; (2) at certain depth (stable cavity depth), soil starts to flow back on top of the spudcan. This keeps the cavity depth unchanged when spudcan penetrates deeper; (3) at deep penetration, the soil flow is fully localised with no effect to the soil surface profile. The deformation of soil field is in the region of 1.3 ~ 1.4 D, which is slightly smaller than that of surface foundation.

The change of soil flow mechanisms at different stages plays a key role in bearing capacity response. The cavity depth has shown a significant influence on bearing capacity factor before the deep embedment soil flow mechanism is reached. However, when the deep flow mechanism occurs, all the analyses converge to a unique N_c value for smooth and rough spudcan respectively. The rough spudcan can provide 14% higher bearing result than that of smooth spudcan. $N_c = 10.5$ for smooth spudcan and 12 for rough spudcan are obtained when spudcan penetrates into uniform soil.

7   Copyright © 2004 by ASME

REFERENCES

[1] Carlsen, C. A., Kjeøy, H., and Eriksson, K., 1986, "Structural Behaviour of Harsh Environment Jack-ups," *The Jack-up Drilling Platform Design and Operation*, London: Collins, pp. 90-136.

[2] Sharples, B. P. M., 1989, "Risk Analysis of Jack-up Rigs," *2nd International Conference, The Jack-up Drilling Platform*, London.

[3] McClelland, B., Young, A. G., and Remmes, B. D., 1981, "Avoiding Jack-up Rig Foundation Failures," *Proc., Symposium on Geotechnical Aspects of Coastal and Offshore Structures*, Bangkok, pp. 137-157.

[4] Young, A. G., Remmes, B. D., and Meyer, B. J., 1984, "Foundation Performance of Offshore Jack-up Drilling Rigs," *Journal of Geotechnical Engineering Division,* ASCE, **110**(7), pp. 841-859.

[5] Craig, W. H., and Chua, K., 1990, "Deep Penetration of Spudcan Foundations on Sand and Clay," *Géotechnique*, **40**(4), pp. 541-556.

[6] Craig, W. H., and Chua, K., 1991, "Large Displacement Performance of Jack-up Spudcans," *Proc., International Conference Centrifuge '91*, Balkema, Rotterdam, pp. 139-144.

[7] Hossain, M. S., Hu, Y., and Randolph, M. F., 2003, "Spudcan Foundation Penetration into Uniform Clay," *Proc., 13th International Offshore and Polar Engineering Conference*, ISOPE, Hawaii.

[8] Dean, E. T. R., James, R. G., Schofield, A. N. and Tsukamoto, Y., 1998, "Drum Centrifuge Study of Three-leg Jackup Models on Clay," *Géotechnique*, **48**(6), pp. 761-785.

[9] Martin, C. M., and Randolph, M. F., 2000, "Application of the Lower and Upper Bound Theorems of Plasticity to Collapse of Circular Foundations," *Report N° G1507*, Geomechanics Group, The University of Western Australia.

[10] Houlsby, G. T., and Martin, C. M., 2003, "Undrained Bearing Capacity Factors for Conical Footings on Clay," *Géotechnique*, **53**(5), pp. 513-520.

[11] Endley, S. N., Rapoport, V., Thompson, P. J., and Baglioni, V. P., 1981, "Prediction of Jack-up Rig Footing Penetration," *Proc., 13th Offshore Technology Conference*, Houston, Texas, OTC 4144, pp. 285-289.

[12] Tirant, P., and Pérol, C., 1993, *Stability and Operation of Jackups*, Technip, Paris.

[13] Stewart, D. P., Boyle, R. S., and Randolph, M. F., 1998, "Experience with a New Drum Centrifuge," *Proc., International Conference Centrifuge '98*, Tokyo, Japan, pp. 35-40.

[14] Carter, J. P., and Balaam, N., 1990, *AFENA User's Manual,* Geotechnical Research Centre, The University of Sydney.

[15] Hu, Y., and Randolph, M. F., 1998, "*H*-Adaptive FE Analysis of Elasto-Plastic Non-Homogeneous Soil with Large Deformation," *International Journal of Computer Geomechanics*, **23**(1), pp. 61-84.

[16] Stewart, D. P., 1992, "Lateral Loading of Pile Bridge Abutments due to Embankment Construction," Ph.D. thesis*, The University of Western Australia.

[17] Stewart, D. P., and Randolph, M. F., 1991, "A New Site Investigation Tool for the Centrifuge," *Proc., International Conference Centrifuge '91*, Balkema, Rotterdam, pp. 531-538.

[18] Finnie, I. M. S., 1993, "Performance of Shallow Foundations in Calcareous Soils," Ph.D. thesis*, The University of Western Australia.

[19] White, D. J., 2002, "An Investigation into the Behaviour of Pressed-in Piles," Ph.D. thesis, Cambridge University.

8   Copyright © 2004 by ASME